The Company of **Biologists**

RESEARCH ARTICLE

Fin and body neuromuscular coordination changes during walking and swimming in *Polypterus senegalus*

Kathleen L. Foster*, Misha Dhuper and Emily M. Standen

ABSTRACT

The ability to modulate the function of muscle is integral to an animal's ability to function effectively in the face of widely disparate challenges. This modulation of function can manifest through short-term changes in neuromuscular control, but also through long-term changes in force profiles, fatiguability and architecture. However, the relative extent to which shorter-term modulation and longer-term plasticity govern locomotor flexibility remains unclear. Here, we obtain simultaneously recorded kinematic and muscle activity data of fin and body musculature of an amphibious fish, *Polypterus senegalus*. After examining swimming and walking behaviour in aquatically raised individuals, we show that walking behaviour is characterized by greater absolute duration of muscle activity in most muscles when compared with swimming, but that the magnitude of recruitment during walking is only increased in the secondary bursts of fin muscle and in the primary burst of the mid-body point. This localized increase in intensity suggests that walking in *P. senegalus* is powered in a few key locations on the fish, contrasting with the more distributed, low intensity muscle force that characterizes the stroke cycle during swimming. Finally, the increased intensity in secondary, but not primary, bursts of the fin muscles when walking probably underscores the importance of antagonistic muscle activity to prevent fin collapse, add stabilization and increase body support. Understanding the principles that underlie the flexibility of muscle function can provide key insights into the sources of animal functional and behavioural diversity.

KEY WORDS: Muscle function, Electromyography, Aquatic, Terrestrial, High-speed videography, Fish

INTRODUCTION

Muscle is responsible for an immense array of tasks integral to the function of animals: its action propels food through digestive tracts, enables birthing, pumps blood through the circulatory system, and powers an enormous range of locomotor behaviours like swimming, jumping and flying. The versatility of muscle enables animals to use existing anatomical machinery to function in new and different ways. Remarkably, muscle functional diversity is accomplished despite the tissue maintaining its basic, fundamental structure.

The ability to modulate functional properties over different time scales is key to allowing muscle to perform such an impressive array of tasks. Over long time frames, either during the lifetime of an animal or through evolutionary time, morphological properties of a muscle, such as size and moment arm, can be altered to affect force production (Alexander, 1977; Sacks and Roy, 1982; Loeb and Gans, 1986; Gans and de Vree, 1987; Payne et al., 2006; Lieber and Ward, 2011; Wilson and Lichtwark, 2011). On a moderate time frame, the efficiency and fatiguability of muscle can be altered through modification of the ratios of different myosin isoforms that define muscle fibre type (Pette and Staron, 2000; Zierath and Hawley, 2004; Schiaffino and Reggiani, 2011) or through alterations to the shape of the force–length curve via changes to the number of sarcomeres (Lynn and Morgan, 1994; Koh, 1997; Koh and Herzog, 1998; Rassier et al., 1999). In the short, virtually instantaneous time frame, behaviour and neuromechanics can be altered to directly affect how the morphology and physiology of the muscle translates into force production. For example, not only can particular motor units and muscle fibre types be used preferentially within a single muscle, but the coordination of muscle activity can be modulated to perform new or complex tasks (Wakeling et al., 2002; Wakeling, 2004; Hodson-Tole and Wakeling, 2009; Foster and Higham, 2014, 2017).

Polypterus senegalus is an amphibious fish that can use its fins and body to locomote effectively in highly disparate environments. Although it prefers to live in water, where it propels itself primarily through oscillations of its pectoral fins, it can live for extended periods on moist land, which dramatically changes the forces experienced by the musculature. When on land, *P. senegalus* employs one of two locomotor gaits: (1) an axial-only gait characterized by lateral undulation of the body in the presence of coarse, irregular substrates that provide lateral surfaces against which it can push, or (2) an axial-appendicular gait (on smooth, flat surfaces), which involves lifting its head and forebody off the ground with its pectoral fins and pivoting around them while pushing forward with the posterior portion of its body (Standen et al., 2016).

Interestingly, *P. senegalus* has demonstrated an ability to respond to being raised on land for extended periods of time through plastic changes to its morphology and locomotor behaviour. After eight months on land, a number of kinematic changes, such as decreased fin slip, more proximal fin placement, and higher nose elevations, suggest that terrestrially raised fish are able to walk more effectively on land than aquatically raised counterparts (Standen et al., 2014). Parallel to these kinematic changes, terrestrially raised *P. senegalus* have stronger connections between clavicle and cleithrum and reduced supracleithrum, indicating a strengthening of the skeletal components of the pectoral girdle and a possible reduction in the association between pectoral girdle and skull (Standen et al., 2014). Furthermore, a recent study has shown increases in the proportion of fast muscle fibre types, especially proximally, in the fins of terrestrially reared *P. senegalus*, compared with aquatically reared fish (Du and Standen, 2017).

Despite evidence for the presence of kinematic and morphological plasticity in *P. senegalus* when raised in a

Department of Biology, University of Ottawa, 30 Marie Curie, Ottawa, ON, K1N 6N5, Canada.

*Author for correspondence (kfoster@uottawa.ca)

K.L.F., 0000-0002-7365-7885

terrestrial environment, it remains unclear what role functional modulation of the neuromuscular system plays in shaping these different locomotor behaviours when confronted with the terrestrial habitat over short or instantaneous time scales. How does modulation of muscle function allow the same morphology to be used in such highly disparate locomotor behaviours when the potential for locomotor or morphological plasticity is limited or absent? Due to the greater importance of gravity in terrestrial than in aquatic environments, we hypothesized increased motor unit recruitment in walking than in swimming *P. senegalus*. Furthermore, we expected that the timing of muscle activity would be closely associated with the timing of kinematic movements, such that shifts in muscle activity patterns would parallel the corresponding shifts in kinematics associated with the two disparate locomotor behaviours.

MATERIALS AND METHODS
Subjects
Nine *Polypterus senegalus* Cuvier 1829 [mass, 4.91±0.66 g; total length (nose to tip of tail), 94.67±4.14 mm] were obtained from the pet trade (Mirdo Importations Canada, Montreal, QC, Canada). Fish were not fed within 24 h prior to surgery to minimize the effect of undigested food on anaesthesia. All procedures were conducted in accordance with the University of Ottawa Animal Care and Use Protocol no. BL-1926-R2 A1.

Surgery and experimental protocol
Fish were anaesthetized in buffered water containing MS-222 (200 mg l^{-1}) for approximately 10 min prior to surgery, and level of anaesthesia was closely monitored throughout surgery to minimize stress/energy expenditure prior to locomotor trials. Bipolar electromyography (EMG) electrodes were constructed from 0.051 mm diameter polycoated stainless-steel wire (California Fine Wire Company, Grover Beach, CA, USA). Electrodes were implanted percutaneously using 26-guage hypodermic needles into left pectoral fin adductor and/or abductor muscles and up to six points along the left and/or right sides of the body (Fig. 1). Because we were interested in examining function of muscles involved in steady swimming behaviours, body electrodes were implanted very shallowly, just dorsal to the lateral line, to ensure that recordings were made of red muscle, as white muscle appears to be only used for burst/fast-start locomotor

behaviours (authors' personal observation). Location of implanted electrodes were confirmed post-experimentation via dissection. Electrodes were tethered to dorsal spines using 5-0 coated vicryl suture (Ethicon, Somerville, NJ, USA) to reduce the potential for electrodes pulling out during trials. After surgery, fish were returned to freshwater in the 10-gallon filming aquarium and allowed to recover until normal, voluntary swimming behaviours returned (0.5 to 1 h post-surgery).

To minimize the impact of EMG implantation on normal aquatic and terrestrial locomotion, we had to limit the number of electrodes implanted according to body size, with fewer electrodes implanted in smaller individuals. We attempted to obtain an even distribution of electrode arrangements by varying the number and location of electrodes between individuals. We used three basic arrangements of electrodes on the body: (1) electrodes implanted at anterior, middle and posterior regions of both sides of the body (points 1, 3 and 5 in Fig. 1A), (2) electrodes implanted equidistantly at five locations (points 1–5 in Fig. 1A) down the left side of the body, and (3) electrodes implanted equidistantly at five locations (points 1–5 in Fig. 1A) down the right side of the body (Fig. 1; see 'Statistical analysis' section for how data were pooled). The electrode implantation locations, along with the number of swimming and 'walking' strokes, can be found in Table S1.

All locomotor trials took place in a 10-gallon aquarium with a plastic floor that remained submerged below approximately 10 cm of water for swimming trials but that could be raised and supported above water level for terrestrial trials. This set-up minimized stress to the animal by eliminating the necessity of handling fish between aquatic and terrestrial trials. Dorsal and lateral videos of aquatic and terrestrial locomotion were obtained through the use of two high-speed Photron Fastcam Mini UX100 (Photron USA, San Diego, CA, USA) cameras recording at 500 frames s^{-1}. Muscle activity data were collected simultaneously and synchronized with the video data via an external trigger. EMG signals were amplified 5000 times and filtered with a 60 Hz notch filter using GRASS P511 AC amplifiers (Natus Neurology, Warwick, RI, USA). Signals were acquired at 10,000 samples s^{-1} using an AD Instruments PowerLab 16/35 data acquisition system (ADInstruments, Colorado Springs, CO, USA), and low- and high-bandpass filters (40–4000 Hz) were applied using LabChart software (version 8.1.1; ADInstruments). Once all trials were complete, fish were killed with an overdose of buffered MS-222 (400 mg l^{-1}).
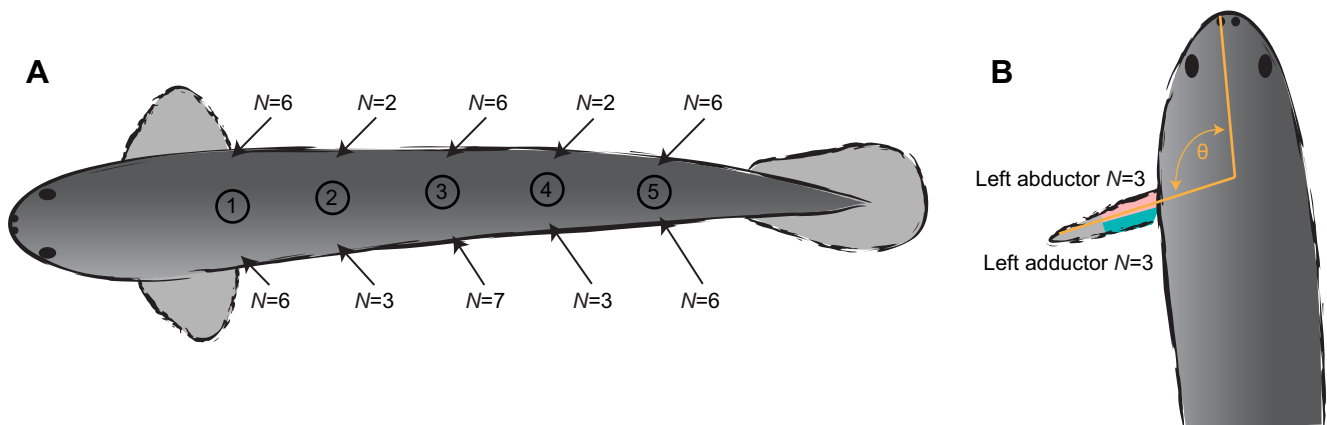

Fig. 1. Schematic showing location of EMG electrode implantation in *Polypterus senegalus*. (A) Body electrodes were implanted just dorsal to the lateral line along the left and/or right sides of the body, spaced equidistantly between pectoral and anal fins, indicated by arrows. (B) Pectoral fin electrodes were implanted in the left adductor (blue) and/or abductor (pink) muscles. N, number of individuals that had an electrode implanted at each location; θ, horizontal fin angle.

Kinematic processing and variables

As a detailed kinematic analysis of walking and swimming *P. senegalus* has already been performed (Standen et al., 2016), all kinematic analyses in the current study are limited to the variables that have the potential to relate most closely to the EMG variables examined. Only strokes and strides that were part of a continuous period of activity were analysed.

Three-dimensional coordinates for the tip of the left pectoral fin and six points along the dorsal aspect of the body (tip of nose, base of head, tip of the tail, and three points spaced equidistantly between the base of the head and the tip of the tail) were obtained using DLTdv5.m custom software (Hedrick, 2008) for MATLAB (version R2017a, The MathWorks, Natick, MA, USA). Movement of the tip of the nose was used to define all aquatic and terrestrial strokes, as described previously; the beginning of the stroke cycle was defined as occurring when the tip of the nose was pointed furthest to one side and the mid-point of the stroke cycle was defined as occurring when the nose was pointed furthest to the opposite side (Standen et al., 2016). This definition of stroke cycle was used to standardize the timing of all temporal kinematic and EMG variables.

Body coordinates were used to create a continuous spline that defined the shape of the body during each frame of video using custom MATLAB code. Using this continuous spline, magnitude and timing of peak wave amplitude (defined as the maximum distance between the path of the fish and the body point) was determined for locations along the body corresponding to the points of EMG implantation. The magnitude of peak body amplitude was standardized as a percentage of body length and the corresponding timing was expressed in polar coordinates (radians) relative to the timing of the stroke cycle (see Dataset 1).

Horizontal fin angle, the angle defined by the tip of the nose, the base of the head, and the tip of the pectoral fin, in the horizontal plane, was calculated such that greater values indicate greater adduction, when the fin is oriented more posteriorly, and smaller values indicate greater abduction, when the fin is oriented more anteriorly (Fig. 1B). From this variable, the maximum and minimum horizontal fin angle, as well as the angular excursion (i.e. delta), were obtained for each fin stroke and the corresponding timing of these variables were expressed relative to the stroke cycle defined by the body. Note that in contrast to walking, where there is a 1:1 ratio of fin to body strokes, swimming *P. senegalus* have approximately two fin strokes for every body stroke, and all fin strokes were standardized to the body stroke cycle (Dataset 1).

Electromyography processing and variables

Bandpass filtered data were used to calculate variables related to the magnitude [peak amplitude and rectified integrated area (RIA) of burst] and timing (burst onset and offset time, duration, timing of peak burst amplitude, and time at which half of the burst RIA was achieved) of muscle activity (see Fig. 2 for representative EMG traces; Dataset 1). All calculations and subsequent statistical analyses were performed using custom MATLAB code.

Background signal noise was subtracted from EMG data and signals were rectified prior to calculations of all EMG magnitude data. Burst RIA was calculated by integrating EMG amplitude over the burst duration and is an indication of the relative proportion of motor units active during the burst. To facilitate comparisons across muscles and individuals, burst RIA was standardized by calculating the theoretical maximum burst RIA for each burst (the product of the burst duration and the maximum amplitude ever observed for that muscle and individual) and expressing burst RIA as a percentage of this theoretical maximum burst RIA. Similarly,

once identified, peak burst amplitude was expressed as a percentage of the maximum amplitude ever observed for that muscle and that individual.

Timing of burst onsets and offsets were determined using methods developed by Roberts and Gabaldón (2008) and described previously (Foster and Higham, 2014, 2017). Briefly, a signal envelope was defined via a 100 Hz low-pass filter, which facilitated identification of the onset and offset points of the bursts, defined as points where the envelope surpassed a pre-determined cut-off value (twice the standard deviation of the inactive EMG signal). Timing of burst onset, offset and peak amplitude were standardized to the polar coordinates of the stroke cycle defined by body kinematics (see above), and thus were expressed in radians. Burst duration, defined as the difference in time between burst onset and offset, was expressed both in absolute time (s) and as a percentage of the duration of the stroke cycle for subsequent analyses. Burst shape was approximated as the time at which half the burst RIA was achieved as a percentage of burst duration (sensu Roberts et al., 2007).

Statistical analyses

As stated above, electrodes were implanted at standardized locations along the body making electrode location equivalent across fish of different body sizes. Left and right side muscle activation patterns were compared for each standardized position along the body and found to be statistically similar. Thus, left and right side data were pooled by body position (using the simple pooling method; Bravata and Olkin, 2001) and mixed-model ANOVAs for red muscle activity variables were conducted for the five points along the length of the body (Fig. 1).

Temporal variables were analysed using circular statistics, as described by Standen et al. (2016). Timing of variables of walking and swimming groups were tested for directionality to determine whether they occurred at the same time in each stroke cycle (Rayleigh's test for directionality). The mean timing (measured in degrees) for variables that showed directionality were compared between walking and swimming groups using Watson–Williams multi-sample tests (Zar, 1999). All timing variables are reported in degrees relative to the beginning of the stroke defined by the motion of the head.

Standard linear statistics were used to compare groups within magnitude variables. Because individual identity is important in our repeated measures experimental design, we performed mixed-model analyses of variance for all our body and fin variables by coding individual as a random factor and manually calculating the correct F statistics using interactions between individual and treatment as error terms, according to Zar (1999). Body and fin data conformed to homoscedasticity requirements by passing Levene's test in 98% of our variables and the number of observations was sufficiently large (>20 for all variables and >30 for most variables; see Table S1 for detailed distribution of data) to render tests of normality unnecessary (Field, 2009; Ghasemi and Zahediasl, 2012).

As we performed a large number of statistical tests, we controlled the false discovery rate (0.05) using the Benjamini–Hochberg method (Benjamini and Hochberg, 1995; McDonald, 2014). All statistical analyses were performed using custom code written in MATLAB.

RESULTS

The activity patterns of both fin and body musculature are characterized by one strong, primary burst and occasionally a
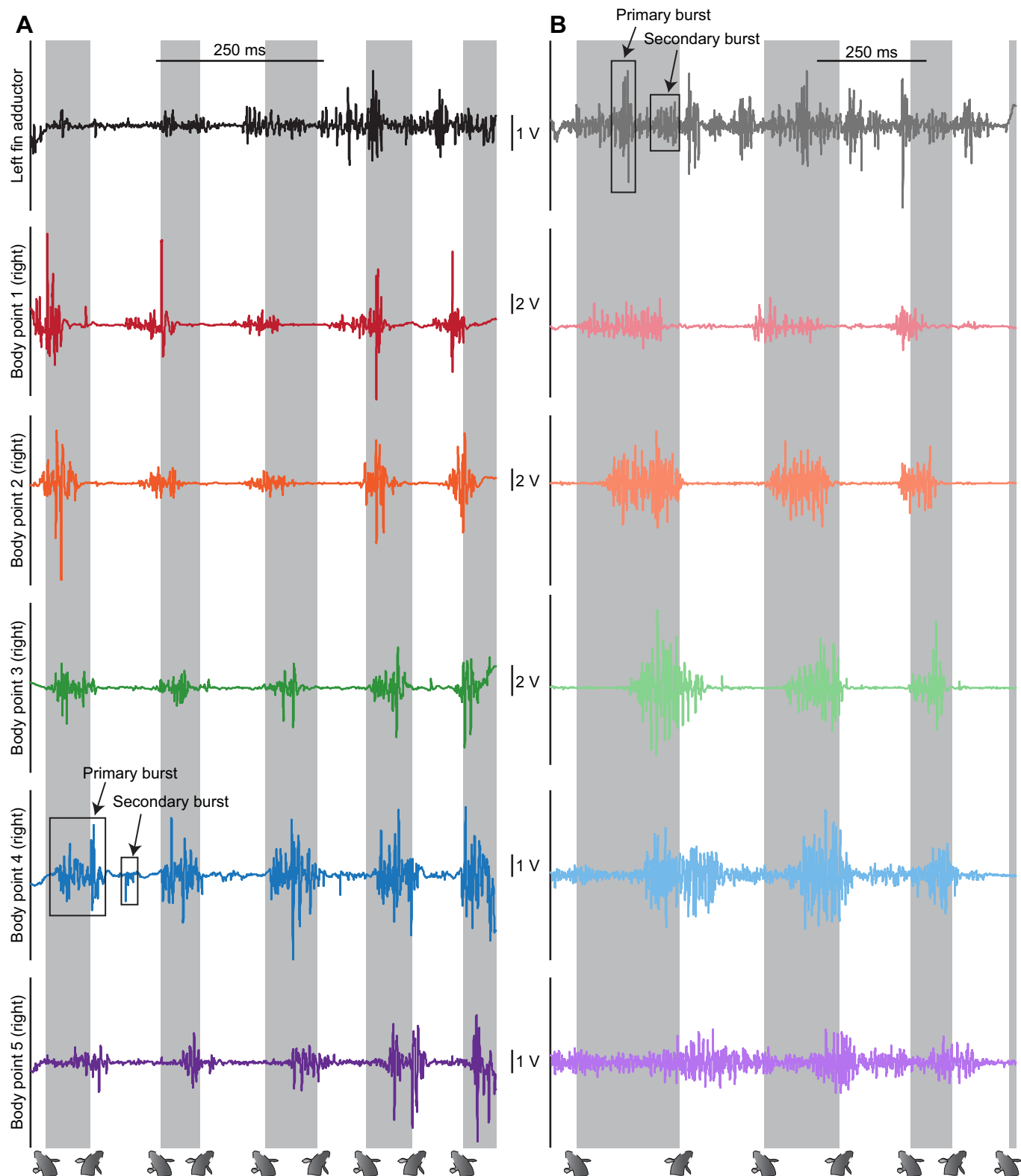
Fig. 2. Example electromyography recordings of the left fin adductor muscle and muscles along the right side of the body of a representative *P. senegalus* swimming and walking. (A) Swimming; (B) walking; grey shaded regions represent the first half of the stroke cycle defined by the head swinging from left to right; unshaded regions represent the second half of the stroke cycle defined by the head swinging from right to left. Body points are identified based on electrode positions defined in Fig. 1. Examples of primary (burst 1) and secondary (burst 2) muscle bursts are indicated with boxes and arrows.

second, smaller burst of activity per stroke. Representative electromyography traces from a single individual swimming and walking can be seen in Fig. 2. The first burst of activity represents

the primary activity of the muscle, coinciding with the generation of movement and often having a considerably greater magnitude and duration than the second burst (if present). The second burst when

Table 1. Results of mixed-model ANOVAs of body kinematic and muscle activity in swimming and walking *Polypterus senegalus*

Variable	Body point	No. individuals	Condition Swim (mean ±s.e.m.)	Walk (mean ±s.e.m.)	ANOVA F-value (d.f.)	ANOVA P-value	Benjamini–Hochberg P-value
Swimming/walking speed (BL s^{-1})		7	1.28±0.06	0.25±0.02	49.64 (1,6)	0.0004*	0.0024*
Wavelength (% BL)		7	54.26±1.42	74.28±1.79	9.97 (1,6)	0.0196*	0.0543
Body stroke duration (s)		7	0.24±0.01	0.55±0.03	18.69 (1,6)	0.0050*	0.0202*
Wave amplitude (% BL)	1	6	2.13±0.14	5.09±0.34	12.57 (1,5)	0.0165*	0.0505
	2	5	2.78±0.21	8.71±0.87	9.64 (1,4)	0.0361*	0.0863
	3	7	3.06±0.16	8.24±0.52	10.84 (1,6)	0.0166*	0.0505
	4	5	4.10±0.26	9.96±1.05	4.87 (1,4)	0.0920	0.1811
	5	7	4.99±0.27	7.34±0.58	2.81 (1,6)	0.1448	0.2419
Wave frequency (s^{-1})	1	6	5.10±0.33	2.19±0.12	10.80 (1,5)	0.0218*	0.0543
	2	5	6.36±0.28	2.10±0.24	36.43 (1,4)	0.0038*	0.0160*
	3	7	4.66±0.24	2.03±0.09	14.12 (1,6)	0.0094*	0.0371*
	4	5	6.59±0.36	2.13±0.26	42.31 (1,4)	0.0029*	0.0140*
	5	7	5.01±0.30	2.15±0.12	13.32 (1,6)	0.0107*	0.0397*
Wave speed (BL s^{-1})	1	5	3.01±0.22	1.29±0.06	13.79 (1,4)	0.0206*	0.0543
	2	5	3.61±0.21	1.55±0.15	41.51 (1,4)	0.0030*	0.0140*
	3	6	2.65±0.17	1.31±0.05	10.80 (1,5)	0.0218*	0.0543
	4	5	3.85±0.39	1.54±0.15	16.13 (1,4)	0.0159*	0.0505
	5	6	3.01±0.21	1.37±0.08	13.98 (1,5)	0.0134*	0.0443*
Max. burst 1 amplitude (% max.)	1	6	23.37±4.77	40.86±3.05	3.09 (1,5)	0.1389	0.2354
	2	5	36.80±6.72	54.89±5.83	1.12 (1,4)	0.3496	0.4739
	3	7	28.32±2.84	51.50±2.95	13.31 (1,6)	0.0107*	0.0397*
	4	5	48.99±5.19	48.05±6.13	0.06 (1,4)	0.8148	0.8796
	5	7	34.64±3.67	48.27±3.88	4.35 (1,6)	0.0820	0.1641
Max. burst 2 amplitude (% max.)	1	6	9.70±2.29	32.78±4.27	2.11 (1,5)	0.2062	0.3225
	2	5	22.46±6.43	31.88±9.43	0.67 (1,4)	0.4596	0.5664
	3	7	22.03±3.96	16.84±2.67	0.001 (1,6)	0.9723	0.9723
	4	5	20.69±6.18	26.93±8.02	0.07 (1,4)	0.8090	0.8796
	5	6	23.38±4.38	10.41±2.07	0.12 (1,5)	0.7467	0.8435
Burst 1 RIA (% max.)	1	6	2.52±0.45	4.92±0.37	5.17 (1,5)	0.0720	0.1515
	2	5	3.26±0.54	6.85±0.72	5.39 (1,4)	0.0810	0.1641
	3	7	3.81±0.42	6.02±0.36	8.31 (1,6)	0.0280*	0.0682
	4	5	6.07±0.79	6.31±0.85	0.81 (1,4)	0.4198	0.5226
	5	7	4.48±0.56	6.43±0.50	3.91 (1,6)	0.0953	0.1846
Burst 2 RIA (% max.)	1	6	1.47±0.39	2.86±0.32	0.08 (1,5)	0.7858	0.8715
	2	5	2.30±0.52	3.27±0.92	0.95 (1,4)	0.3845	0.5155
	3	7	2.56±0.39	2.17±0.35	0.05 (1,6)	0.8258	0.8837
	4	5	2.19±0.57	3.23±1.13	0.62 (1,4)	0.4744	0.5731
	5	6	3.09±0.71	1.37±0.17	0.39 (1,5)	0.5611	0.6582
t half burst 1 RIA (% burst duration)	1	6	49.55±2.32	53.69±1.03	1.87 (1,5)	0.2299	0.3463
	2	5	48.06±2.45	53.54±1.85	4.60 (1,4)	0.0987	0.1862
	3	7	50.61±1.61	52.92±0.95	0.78 (1,6)	0.4115	0.5226
	4	5	46.33±1.98	46.76±2.13	0.01 (1,4)	0.9223	0.9427
	5	7	51.17±1.98	47.25±0.98	1.16 (1,6)	0.3231	0.4539
t half burst 2 RIA (% burst duration)	1	6	47.54±1.78	44.53±1.65	0.04 (1,5)	0.8585	0.9035
	2	5	41.58±2.97	47.37±2.34	7.96 (1,4)	0.0478*	0.1080
	3	7	45.68±1.84	48.42±1.05	1.10 (1,6)	0.3342	0.4582
	4	5	49.35±2.27	48.18±2.10	0.02 (1,4)	0.8858	0.9159
	5	6	49.76±2.92	47.76±1.22	0.01 (1,5)	0.9273	0.9427
Burst 1 duration (% stroke duration)	1	6	43.65±3.37	47.23±2.00	0.18 (1,5)	0.6887	0.7927
	2	5	50.18±3.47	35.71±2.69	6.62 (1,4)	0.0618	0.1371
	3	7	51.34±4.40	42.70±1.34	2.22 (1,6)	0.1866	0.2956
	4	5	55.09±2.90	38.08±2.95	8.47 (1,4)	0.0436*	0.1024
	5	7	46.66±2.57	40.78±1.66	4.93 (1,6)	0.0682	0.1460
Burst 2 duration (% stroke duration)	1	6	35.84±4.00	38.57±4.01	0.03 (1,5)	0.8590	0.9035
	2	5	43.76±5.67	29.72±3.59	6.29 (1,4)	0.0663	0.1444
	3	7	46.42±9.68	27.76±1.86	1.74 (1,6)	0.2352	0.3500
	4	5	37.54±3.54	26.38±2.36	4.57 (1,4)	0.0992	0.1862
	5	6	44.68±2.80	27.48±1.49	11.25 (1,5)	0.0202*	0.0543
Burst 1 duration (s)	1	6	0.09±0.01	0.22±0.01	31.13 (1,5)	0.0025*	0.0130*
	2	5	0.09±0.004	0.20±0.02	13.92 (1,4)	0.0203*	0.0543
	3	7	0.12±0.02	0.22±0.01	1.87 (1,6)	0.2203	0.3402
	4	5	0.09±0.005	0.21±0.02	14.10 (1,4)	0.0199*	0.0543
	5	7	0.10±0.01	0.20±0.01	9.48 (1,6)	0.0217*	0.0543

Table 1. Continued

Variable	Body point	No. individuals	Condition		ANOVA F-value (d.f.)	ANOVA P-value	Benjamini–Hochberg P-value
			Swim (mean ±s.e.m.)	Walk (mean ±s.e.m.)			
Burst 2 duration (s)	1	6	0.07±0.01	0.18±0.01	26.88 (1,5)	0.0035*	0.0153*
	2	5	0.07±0.01	0.15±0.02	18.46 (1,4)	0.0127*	0.0430*
	3	7	0.11±0.03	0.14±0.01	0.11 (1,6)	0.7550	0.8451
	4	5	0.06±0.01	0.17±0.03	4.48 (1,4)	0.1018	0.1881
	5	6	0.10±0.01	0.13±0.01	3.22 (1,5)	0.1325	0.2277
t peak body amplitude – t burst 1 onset (deg)	1	6	184.30±14.46	154.03±19.28	0.62 (1,5)	0.4668	0.5695
	2	5	234.22±19.95	131.29±20.81	3.74 (1,4)	0.1253	0.2184
	3	7	219.15±9.59	114.21±5.88	29.95 (1,6)	0.0016*	0.0082*
	4	5	252.61±16.57	136.00±27.12	18.50 (1,4)	0.0126*	0.0430*
	5	7	232.00±9.77	154.30±10.26	4.36 (1,6)	0.0818	0.1641
t peak body amplitude – t max. burst 1 amplitude (deg)	1	6	84.18±16.89	−25.89±11.80	6.94 (1,5)	0.0463*	0.1065
	2	5	64.75±32.86	8.19±27.74	2.54 (1,4)	0.1863	0.2956
	3	7	101.13±14.89	26.71±4.84	3.66 (1,6)	0.1042	0.1898
	4	5	79.57±24.57	44.19±21.79	0.82 (1,4)	0.4168	0.5226
	5	7	46.74±22.34	63.27±10.50	0.50 (1,6)	0.5065	0.6058

Individual was coded as a random factor in the models. Numerator and denominator d.f. are given in parentheses after F-values. Significant differences are indicated with an asterisk. BL, body lengths; max., maximum; RIA, rectified integrated area; t, time.

present, coincides temporally with the primary burst of antagonistic muscles, suggesting a stabilizing function. Note that we are unable to distinguish between the presence of a very low intensity secondary burst and the complete absence of the secondary burst. Although it would be interesting from a neural control perspective to know whether a primary/secondary burst structure of varying intensity is always present, we would argue that a signal of undetectable intensity has little effect on the functional output of the muscle.

Body kinematics and muscle activity
The posteriorly directed wave of deflections of the body during walking and swimming was generated by activity of the axial muscles that progressed in waves that travelled posteriorly down the length of the fish. The first half of the stroke, defined by the nose swinging from left to right, involved sequential primary bursts of activity of the axial muscles on the right side of the body, which resulted in the corresponding section of the body bending to the right. Similarly, the second half of the stroke, when the nose was swinging from right to left, featured the primary bursts of the left axial muscles. Secondary bursts for a given side, when observed, generally occurred during a portion of the primary burst of the contralateral side.

Fish moved at slower speeds and the wave that moved posteriorly down the body had a lower frequency and slower wave speed in walking compared with swimming fish (Table 1). At body point 3, maximum amplitude of the first muscle burst was significantly greater in walking than in swimming fish, but there was no significant difference at any other location on the body (Table 1, Fig. 3B,C). The duration of the first burst of muscle activity, in absolute time, was significantly greater at body point 1 for walking compared with swimming fish, and the duration of the second burst of activity was greater when walking than when swimming at the first two body points (Table 1; Fig. 3E,F). When expressed as a percentage of stroke duration, these significant differences disappeared (Table 1; Fig. 3D).

The body wave reached peak amplitude significantly earlier in walking than in swimming at almost all locations down the body (Table 2, Fig. 4A). In contrast, the onset time, offset time, and maximum amplitude of burst 1 muscle activity took place later in the stroke cycle in walking than in swimming fish (Table 2, Fig. 4B). Together these data resulted in muscle activity occurring significantly closer to the timing of peak body amplitude in walking than in swimming fish at body points 3 and 4, although this difference was non-significant at the other body points (Table 1, Fig. 4C,D). The timing of the second burst of muscle activity was not directional (i.e. it failed Rayleigh's test) at almost every point along the body, indicating that the timing of the second burst of activity, when observed, was highly variable (Table 2).

Fin kinematics and muscle activity
There is a significantly greater range of motion of the pectoral fin during walking than swimming (Table 3, Fig. 5). This greater range of motion did not appear to result from greater primary burst activity in adductor or abductor muscles (Fig. 6A,B). The maximum amplitude of the second burst of the abductor muscle was significantly greater in walking than in swimming fish (Table 3, Fig. 6E).

The timing of maximum fin abduction occurred later in the stroke and maximum fin adduction occurred earlier in the stroke during walking compared with swimming (Table 4). This change in fin beat time during walking was less than 1% of the stroke cycle duration and did not translate to differences in fin adductor or abductor muscle activity timing (Table 4).

DISCUSSION
Through the simultaneous recording of high-speed video and electromyography data, we found significant shifts in kinematics and muscle activity in *P. senegalus* swimming in water versus walking on land.

Environment alters the magnitude of muscle recruitment
The physical environment through which animals move can have a profound impact on their locomotor behaviour as well as on the muscles that power those behaviours. For example, numerous studies have found increased motor unit recruitment in the muscles of animals moving up steeper inclines (e.g. cats, Carlson-Kuhta et al., 1998; turkeys, Gabaldón et al., 2001; rats, Gillis and Biewener, 2002;
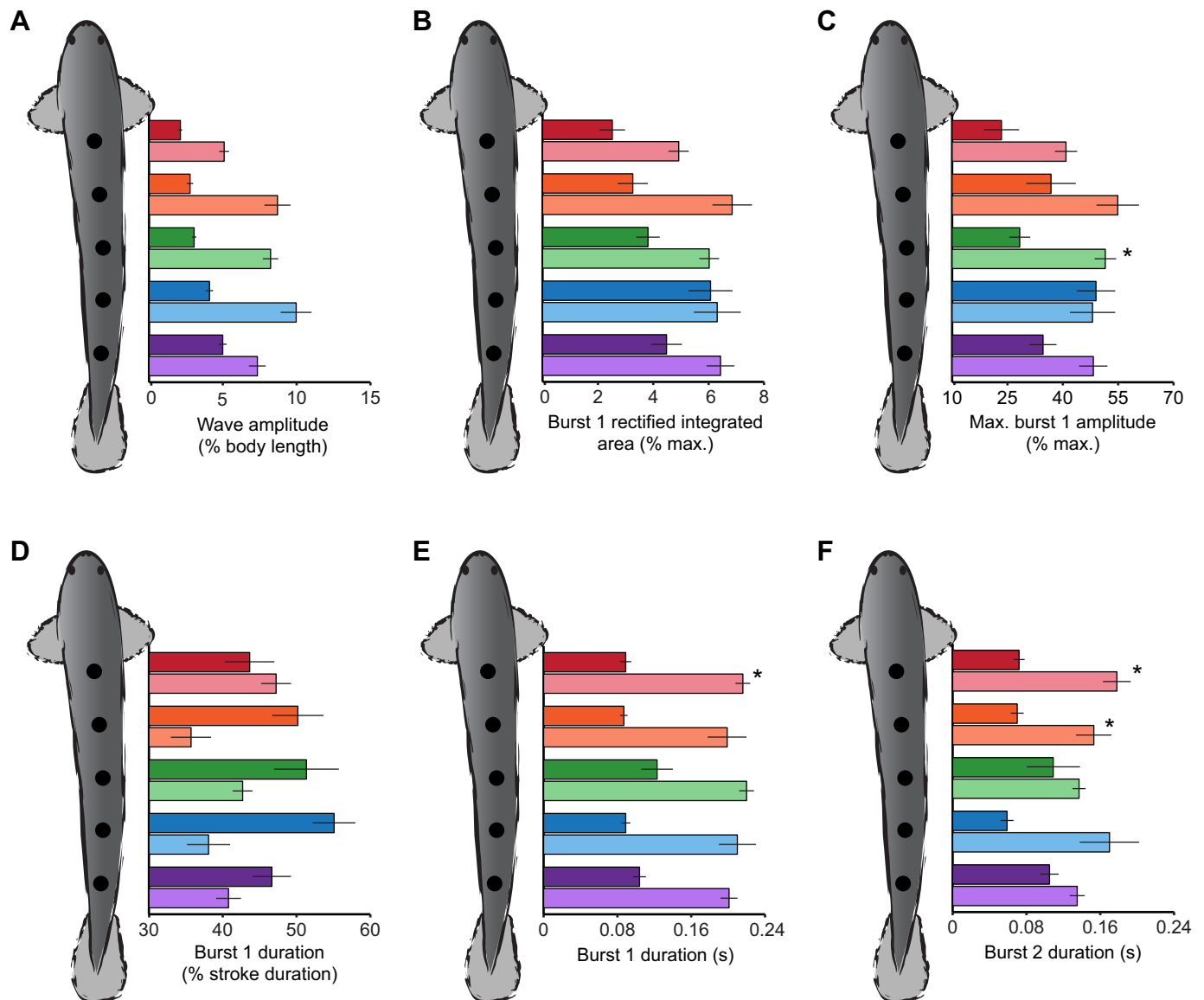
Fig. 3. Differences in kinematic and muscle activity of body magnitude variables. (A) Wave amplitude, expressed as a percentage of body length. (B) Rectified integrated area (RIA) of first muscle burst, expressed as a percentage of maximum burst RIA. (C) Maximum amplitude of first muscle burst, expressed as a percentage of maximum amplitude ever observed for each muscle and individual. (D) Duration of first muscle burst, expressed as a percentage of the duration of the body stroke. (E) Duration of the first muscle burst, in seconds. (F) Duration of the second muscle burst, in seconds. Values are means±s.e.m. Colours correspond to the points along the body, anterior to posterior, consistent with Fig. 2. Deeper shades represent swimming, paler shades represent walking. Asterisks indicate significant differences between swimming and walking treatments (see Table 2 for *P*-values). Positions of the graphs along the body of the fish correspond to electrode implantation locations (see Fig. 1A).

guineafowl, Daley and Biewener, 2003; chameleons, Higham and Jayne, 2004; and Anolis lizards, Foster and Higham, 2014; Foster and Higham, 2017). Similar increases in recruitment are seen in animals moving from the viscous, supportive aquatic environment to terrestrial substrates dominated by gravitational forces (e.g. eels, Gillis, 2000; toads, Gillis and Biewener, 2000; and rats, Gillis and Blob, 2001). Such increases in recruitment result in the greater force and work production necessary to combat the increased resistive component of gravity (Cartmill, 1985; Gillis and Biewener, 2002; Preuschoft, 2002; Daley and Biewener, 2003). When walking on land, *P. senegalus* increased fin and mid-body muscle recruitment (burst RIA and maximum burst amplitude) by 1.5–2 times that during swimming in water (Tables 1 and 3; Figs 3B,C and 6C–E). The absolute time fin and body muscles were active was longer for

walking compared with swimming (approximately two times greater in body muscles and at least four times greater in fin muscles; Tables 1 and 3; Figs 3E,F and 6G,H). These differences were not always statistically significant after correction for multiple tests; given the magnitude of the differences between groups, the near significance of the majority of the Benjamini–Hochberg *P*-values ($P<0.06$), and the conservative nature of corrections for multiple comparisons, there may be a functional significance in the combined subtle changes in these variables. These changes in muscle effort and activation timing suggest that terrestrial environment affects muscle performance by requiring larger muscle output in terrestrial environments.

The effect of walking on muscle recruitment allows us to formulate hypotheses about how the fish were coordinating body and fins to navigate the very different mechanical forces of a novel

Table 2. Results of Watson–Williams multi-sample tests of body kinematic and muscle activity timings in swimming and walking *P. senegalus*

Variable	Body point	No. individuals	Swim Angular mean ±angular variance	Swim Rayleigh *P*-value	Walk Angular mean ±angular variance	Walk Rayleigh *P*-value	Watson–Williams *F*-value (d.f.)	Watson–Williams *P*-value	Benjamini–Hochberg *P*-value
t peak body amplitude (deg)	1	7	123.72±55.03	<0.0001	75.66±67.71	0.0001	59318.25 (1,128)	<0.0001*	<0.0001*
	2	5	230.74±34.51	<0.0001	252.71±59.13	0.0078	532.88 (1,47)	<0.0001*	<0.0001*
	3	7	253.01±74.13	<0.0001	238.54±56.04	<0.0001	12007.95 (1,163)	<0.0001*	<0.0001*
	4	5	293.57±60.42	0.0009	291.15±96.73	0.6206	n/a	n/a	n/a
	5	7	346.58±73.78	<0.0001	299.23±80.54	0.0087	54874.02 (1,122)	<0.0001*	<0.0001*
t burst 1 onset (deg)	1	6	279.36±78.02	0.0413	33.10±36.20	<0.0001	36001.52 (1,68)	<0.0001*	<0.0001*
	2	5	29.65±60.17	0.0246	144.12±70.61	0.2007	n/a	n/a	n/a
	3	7	14.65±71.38	0.0002	120.34±41.59	<0.0001	183902.40 (1,113)	<0.0001*	<0.0001*
	4	5	26.80±43.33	0.0002	148.37±93.03	0.6397	n/a	n/a	n/a
	5	7	92.51±44.25	<0.0001	122.28±45.34	<0.0001	7295.74 (1,89)	<0.0001*	<0.0001*
t burst 1 offset (deg)	1	6	83.53±40.03	<0.0001	177.97±41.22	<0.0001	38024.09 (1,74)	<0.0001*	<0.0001*
	2	5	169.08±41.56	0.0005	278.59±36.57	0.0067	1971.60 (1,25)	<0.0001*	<0.0001*
	3	7	159.22±60.85	<0.0001	287.51±35.59	<0.0001	233121.10 (1,111)	<0.0001*	<0.0001*
	4	5	233.77±48.52	0.0017	340.76±39.63	0.0039	2945.76 (1,28)	<0.0001*	<0.0001*
	5	7	245.59±68.04	0.0005	298.17±35.66	<0.0001	18500.73 (1,82)	<0.0001*	<0.0001*
t burst 2 onset (deg)	1	6	187.79±46.35	<0.0001	195.12±77.08	0.0224	149.68 (1,59)	<0.0001*	<0.0001*
	2	5	304.00±61.92	0.0492	19.75±68.28	0.2351	n/a	n/a	n/a
	3	7	351.71±86.26	0.1174	353.48±51.66	<0.0001	n/a	n/a	n/a
	4	5	331.86±71.65	0.1402	36.01±51.05	0.0421	n/a	n/a	n/a
	5	6	347.52±101.56	0.6149	334.64±31.52	<0.0001	n/a	n/a	n/a
t burst 2 offset (deg)	1	6	267.70±105.82	0.8763	321.13±71.38	0.0111	n/a	n/a	n/a
	2	5	163.05±64.81	0.1249	139.34±77.09	0.4376	n/a	n/a	n/a
	3	7	307.75±93.09	0.3633	63.68±40.39	<0.0001	n/a	n/a	n/a
	4	5	1.85±76.85	0.2481	127.31±97.74	0.8490	n/a	n/a	n/a
	5	6	99.66±93.27	0.3105	63.11±32.72	<0.0001	n/a	n/a	n/a
t max. burst 1 amplitude (deg)	1	6	4.99±51.33	<0.0001	107.31±45.35	<0.0001	46926.34 (1,74)	<0.0001*	<0.0001*
	2	5	74.18±39.77	0.0006	195.23±46.44	0.0249	2101.40 (1,24)	<0.0001*	<0.0001*
	3	7	74.85±61.04	<0.0001	205.88±44.08	<0.0001	264421.62 (1,112)	<0.0001*	<0.0001*
	4	5	126.12±42.08	0.0001	228.39±83.78	0.4613	n/a	n/a	n/a
	5	7	167.09±61.42	<0.0001	199.41±56.08	<0.0001	7334.38 (1,81)	<0.0001*	<0.0001*
t max. burst 2 amplitude (deg)	1	6	238.70±75.90	0.0635	247.42±75.67	0.0237	n/a	n/a	n/a
	2	5	29.00±73.27	0.2132	76.21±87.21	0.6107	n/a	n/a	n/a
	3	7	67.21±103.65	0.7497	30.99±55.03	<0.0001	n/a	n/a	n/a
	4	5	35.70±95.88	0.6959	68.81±55.52	0.0669	n/a	n/a	n/a
	5	6	87.97±109.86	0.9413	15.89±28.20	<0.0001	n/a	n/a	n/a

Numerator and denominator d.f. are given in parentheses after *F*-values. Significant differences are indicated with an asterisk. When Rayleigh's test did not indicate significant directionality for both swimming and walking conditions, Watson–Williams test were not performed. *t*, time; n/a, not applicable.

terrestrial environment. The mid-body (point 3) appeared to be coordinating with the fins to provide the propulsive burst required to hoist the body over the fin. While the magnitude of mid-body muscle recruitment increased during walking (maximum amplitude was significantly greater with *P*=0.0397 and RIA was nearly significant with *P*=0.0682), these increases were not significant in the rest of the body (*P*=0.1515–8796; Table 1, Fig. 3B,C). In contrast, all body muscles except the mid-body muscles increased the duration of muscle activity during walking [significantly in body point 1 (*P*=0.0130) and nearly significantly in body points 2, 4 and 5 (*P*=0.0543)], whereas this increase in duration was not significant in the mid-body muscle (*P*=0.3402; Table 1, Fig. 3E). In this way it appears that the body is partitioned, the mid-body providing propulsion and the anterior and posterior portions of the body stiffening for longer periods of time, possibly in a supportive role. Casual observation of the walking behaviour supports this theory, although quantification of the force profiles generated by the different positions of the body would be highly informative.

During a single locomotory cycle, muscle can have a primary and secondary burst of activity. The secondary burst of fin muscle activity appeared to be more strongly affected by changes in locomotor behaviour than the primary burst of activity. Traditionally, primary muscle bursts are thought to be associated with generating most of the locomotor movements that we observe, leaving secondary bursts to be responsible for antagonistic and/or stabilizing functions (Reilly, 1995; Gatesy, 1997; Higham and Jayne, 2004; Foster and Higham, 2014). Secondary bursts have been noted as having a stabilizing function in locomotion (Gatesy, 1997). The increase in the maximum amplitude of the secondary bursts in fin abductor and adductor muscle in *P. senegalus* suggest that the fin is playing a larger supportive role during walking compared with swimming (abductor: walking amplitude was 3.2 times swimming amplitude, *P*=0.0430; adductor: walking amplitude was 2.1 times swimming amplitude, *P*=0.1915). An increase in fin muscle activity during the secondary burst may help support the body, preventing collapse and enabling the fins to function as pivot points during the walking behaviour.

Environment alters the temporal relationship between muscle activity and kinematics

The absolute duration of body muscle activity increased during walking compared with swimming [significantly at the most
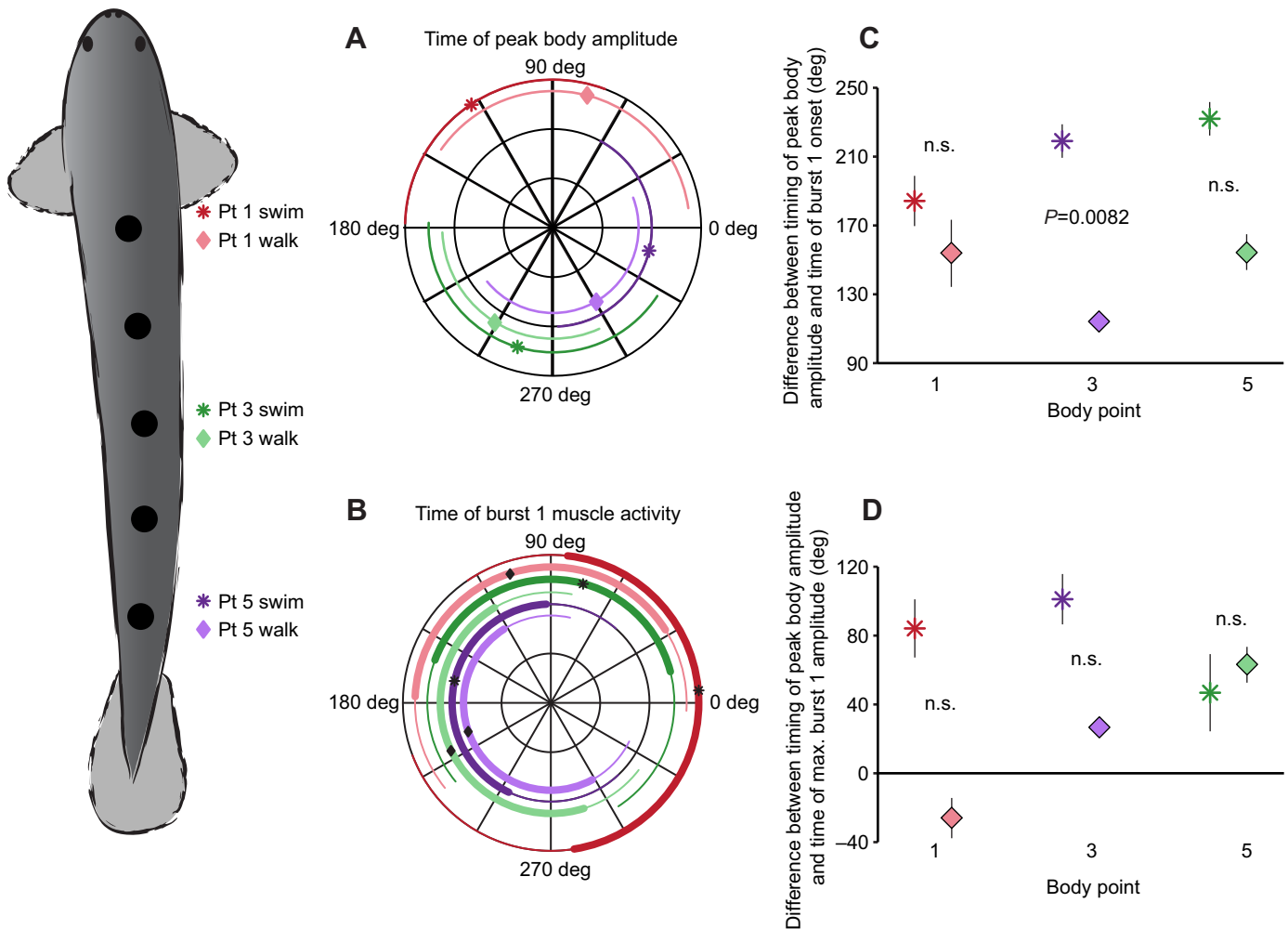
Fig. 4. Differences in kinematic and muscle activity of body timing variables at body electrodes implanted at locations 1, 3 and 5, combined for both sides of the body. Pt, body point location. (A) Polar plot of timing of peak body amplitude. (B) Polar plot of timing of burst 1 muscle activity. Thick bars indicate time during which muscle is active, from angular mean of onset to angular mean of offset. Narrow bars indicate angular variance of onset and offset times. Asterisks and diamonds indicate angular mean time of maximum burst 1 amplitude for swimming and walking, respectively. (A,B) Beginning of the stroke is 0 deg, mid-stroke is 180 deg, and the stroke progresses in a counterclockwise direction. Values are angular means±angular variance. Radial position of the points has no significance and is only meant to improve clarity of presentation. See Table 2 for details of statistical tests. (C) Timing of peak body amplitude minus timing of the onset of the first muscle burst. (D) Timing of peak body amplitude minus timing of the maximum amplitude of the first muscle burst. (C,D) Values greater or less than zero indicate that muscle activity variable occurs before or after the time of peak body amplitude, respectively. Values close to zero indicate that muscle activity variable occurs close to the time of peak body amplitude. Values are means±s.e.m. Benjamini–Hochberg P-values are given where significant differences between swimming and walking exist. n.s., not significant. See Table 1 for details of statistical tests. (A–D) Red, green and purple indicate values at anterior, middle and posterior positions on the body, respectively, and match colours of the corresponding points in Fig. 2. Deeper shades represent swimming, paler shades represent walking.

anterior body point (P=0.0130) and nearly significantly in body points 2, 4 and 5 (P=0.0543)] but represented a similar or slightly smaller proportion of the propulsive stroke. The significantly increased stroke duration of walking (0.55±0.03 s, mean±s.e.m.) compared with swimming (0.24±0.01 s, mean±s.e.m.) explains this discrepancy. More importantly, because the increased duration of muscle activity during walking was accompanied by a much larger range of motion in the anterior body points (body wave amplitude was 2.4–3.1 times greater in walking than in swimming at body points 1–3, P=0.0505–0.0863; Table 1, Fig. 3A), the muscle was probably operating over a greater range of muscle lengths, which can have profound implications on the force production capacity of these muscles (Azizi, 2014; Thompson et al., 2014; Holt and Azizi, 2016; Foster and Higham, 2017).

Indeed, the increase in magnitude of recruitment in the fins and middle body point in walking compared with swimming trials

suggests a requirement for increased force production. In the mid-body muscles, the maximum amplitude of the primary muscle burst was significantly larger [and RIA (P=0.0682) trended towards being larger] in walking compared with swimming fish (Table 1, Fig. 3B–F). Furthermore, when walking, activity of the mid-body musculature occurred later in the stroke, resulting in the onset of muscle activity occurring closer to the timing of peak body amplitude (Tables 1 and 2, Fig. 4B,C). In summary, walking behaviours are generated by more intense bursts of mid-body and fin muscle activity, whereas swimming behaviours are powered by more moderate muscle activity in fins and all along the body.

In general, although shifts in the timing of muscle activity relative to movement are less common than shifts in magnitude when animals are faced with changes in environmental demand, they have been observed in several species [e.g. eels (Biewener and Gillis, 1999); guineafowl (Daley and Biewener, 2003); and *Anolis* lizards

Table 3. Results of mixed-model ANOVAs of fin kinematic and muscle activity magnitudes in swimming and walking *P. senegalus*

Variable	Fin muscle	No. individuals	Swim (mean ±s.e.m.)	Walk (mean ±s.e.m.)	ANOVA F-value (d.f.)	ANOVA P-value	Benjamini–Hochberg P-value
Fin stroke duration (s)		6	0.12±0.005	0.58±0.05	27.63 (1,5)	0.0033*	0.0149*
Min. horizontal fin angle (deg)		6	128.11±2.53	89.64±3.13	12.10 (1,5)	0.0177*	0.0526
Max. horizontal fin angle (deg)		6	155.78±2.49	167.40±2.00	1.35 (1,5)	0.2972	0.4316
Delta horizontal fin angle (deg)		6	27.67±1.02	77.76±3.21	50.96 (1,5)	0.0008*	0.0046*
Fin stroke frequency (s^{-1})		6	9.10±0.33	2.06±0.15	70.17 (1,5)	0.0004*	0.0024*
Max. burst 1 amplitude (% max.)	Adductor	2	38.04±5.51	33.95±6.37	5.07 (1,1)	0.2661	0.3911
	Abductor	2	34.99±5.07	55.50±8.14	1.89 (1,1)	0.4000	0.5226
Max. burst 2 amplitude (% max.)	Adductor	2	20.54±2.84	43.35±5.86	33.89 (1,1)	0.1083	0.1915
	Abductor	2	10.46±1.49	33.43±10.94	2780.02 (1,1)	0.0121*	0.0430*
Burst 1 RIA (% max.)	Adductor	2	7.09±1.04	4.91±1.11	0.24 (1,1)	0.7114	0.8112
	Abductor	2	5.63±0.67	4.82±0.96	0.003 (1,1)	0.9652	0.9723
Burst 2 RIA (% max.)	Adductor	2	3.97±0.42	6.50±1.17	14.73 (1,1	0.1623	0.2640
	Abductor	2	2.45±0.34	3.26±1.05	7.22 (1,1)	0.2268	0.3458
Burst 1 duration (% stroke duration)	Adductor	2	53.28±3.78	34.47±3.10	3.54 (1,1)	0.3110	0.4463
	Abductor	2	50.39±3.80	49.40±5.95	0.75 (1,1)	0.5449	0.6455
Burst 2 duration (% stroke duration)	Adductor	2	42.31±3.12	31.03±3.91	15.93 (1,1)	0.1563	0.2576
	Abductor	2	37.09±3.62	30.16±10.81	0.04 (1,1)	0.8720	0.9093
Burst 1 duration (s)	Adductor	2	0.06±0.005	0.26±0.08	1.71 (1,1)	0.4154	0.5226
	Abductor	2	0.06±0.01	0.24±0.04	34.60 (1,1)	0.1072	0.1915
Burst 2 duration (s)	Adductor	2	0.05±0.004	0.21±0.05	3.17 (1,1)	0.3259	0.4539
	Abductor	2	0.04±0.005	0.16±0.05	2.03 (1,1)	0.3897	0.5168
t half burst 1 RIA (% burst duration)	Adductor	2	45.32±1.83	46.17±3.74	0.09 (1,1)	0.8102	0.8796
	Abductor	2	50.06±2.18	42.77±4.44	0.37 (1,1)	0.6530	0.7588
t half burst 2 RIA (% burst duration)	Adductor	2	51.31±2.25	45.62±2.94	3.13 (1,1)	0.3274	0.4539
	Abductor	2	41.85±2.02	47.79±1.17	1.79 (1,1)	0.4084	0.5226

Individual was coded as a random factor in the models. Numerator and denominator d.f. are given in parentheses after F-values. Significant differences are indicated with an asterisk.

(Foster and Higham, 2014)]. Similar to what we found in *P. senegalus*, the body muscles of eels moving on land had longer EMG burst durations, in absolute time, and the timing of onset of muscle activity was shifted to later in the stroke compared with swimming individuals (Biewener and Gillis, 1999). However, in eels, the duration of muscle activity as a proportion of stroke duration was longer during terrestrial locomotion compared with aquatic locomotion. Muscle activity during more of the stroke cycle suggests that muscles have a more continuous function during terrestrial locomotion in eels compared with *P. senegalus*, which show no changes between locomotion styles (Biewener and Gillis, 1999). This discrepancy between species may be related to the supportive role of pectoral fins in terrestrial locomotion in *P. senegalus* compared with the apparent lack of fin use in eels. Changes in muscle activation timing relative to corresponding kinematics determine whether a muscle absorbs or produces work

and where on its force–length curve it operates, having a profound impact on its contribution to the locomotor effort (Roberts et al., 1997; Rassier et al., 1999; Foster and Higham, 2017). However, how the present changes in motor unit recruitment affect muscle force and work production must remain speculative until force–length properties and *in vivo* muscle length changes can be characterized.

In *P. senegalus*, the changes in the activity patterns of fin and body muscles are probably responsible for the increased range of motion observed in both body and fins during walking compared with swimming. Not only was the amplitude of the wave travelling down the body greater in walking than in swimming fish (2.4–3.1 times greater at body points 1–3, $P=0.0505$–0.0863; Table 1; Fig. 3A), but increases (though insignificant) in both adduction and abduction of the pectoral fin resulted in significantly greater total angular excursion of the fin ($P=0.0046$; Table 3; Fig. 5).
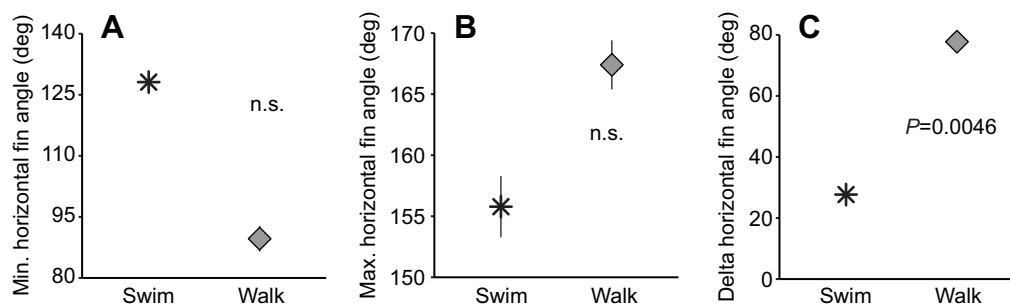

Fig. 5. Differences in magnitudes of pectoral fin kinematic variables. (A) Minimum horizontal fin angle in degrees. Smaller and larger values indicate increased and decreased fin abduction, respectively. (B) Maximum horizontal fin angle in degrees. Smaller and larger values indicate decreased and increased fin adduction, respectively. (C) Horizontal angular excursion of the pectoral fin, calculated as the difference between maximum and minimum horizontal fin angles. Black asterisks and grey diamonds represent swimming and walking treatments, respectively, corresponding to the shading in Fig. 2 and symbols in the other figures. Values are means±s.e.m. Benjamini–Hochberg P-values are given in each panel. n.s., not significant. See Table 3 for details of statistical tests.
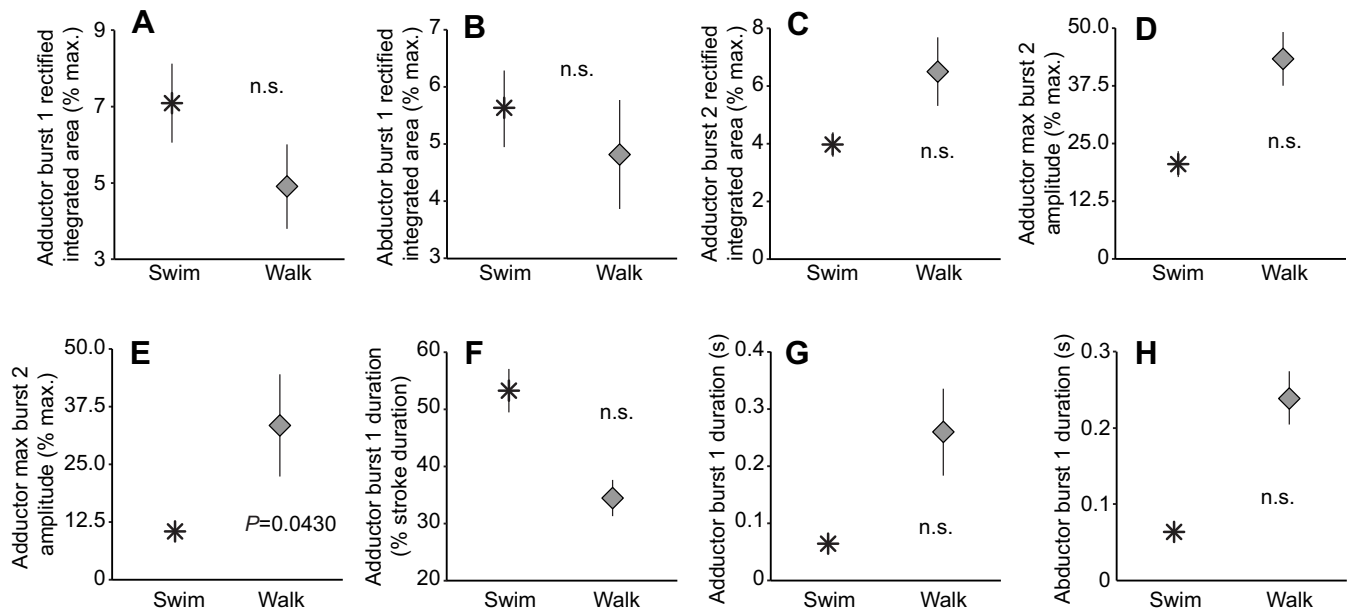
Fig. 6. Differences in muscle activity of pectoral fin magnitude variables. (A) Rectified integrated area of the first burst of the adductor muscle. (B) Rectified integrated area of the first burst of the abductor muscle. (C) Rectified integrated area of the second burst of the adductor muscle. (D) Maximum amplitude of the second burst of the adductor muscle. (E) Maximum amplitude of the second burst of the abductor muscle. (F) Duration of the first burst of the abductor muscle, expressed as a percentage of fin stroke duration. (G) Duration of the first burst of the adductor muscle, in seconds. (H) Duration of the first burst of the abductor muscle, in seconds. Black asterisks and grey diamonds represent swimming and walking treatments, respectively, corresponding to the shading in Fig. 2 and symbols in the other figures. Values are means±s.e.m. Benjamini–Hochberg P-values are given where significant differences between swimming and walking exist. n.s., not significant. See Table 3 for details of statistical tests.

Such increases in movement are probably due to a combination of greater magnitude (Figs 3B,C and 6C–E) and/or absolute duration (Figs 3E,F and 6G,H) of muscle activity in both the pectoral fin and axial muscles. Furthermore, during walking, there was a portion of the stroke (approximately one-sixth of stroke cycle) when all ipsilateral axial muscles were active at the same time, along the entire length of the fish and with especially long overlap in the activity of the posterior muscles of the fish. In contrast, the anterior-most muscle was not active at the same time as the posterior-most muscle during swimming (Fig. 4B). The greater overlap of axial muscle activity during walking probably plays a considerable role in

generating the greater wave amplitudes and characteristic C-shapes that the fish achieves compared with the smaller body deflections inherent in swimming.

Plasticity and other physiological considerations
Polypterus senegalus raised in terrestrial environments for extended periods demonstrated changes in pectoral muscle and skeletal morphology and locomotory kinematics: morphological and behavioural plasticity (Standen et al., 2014; Du and Standen, 2017). How these terrestrialized animals changed their muscle activation patterns to accomplish these new behaviours is unknown.

Table 4. Results of Watson–Williams multi-sample tests of fin kinematic and muscle activity timings in swimming and walking *P. senegalus*

Variable	Fin muscle	No. individuals	Swim Angular mean ±angular variance	Swim Rayleigh P-value	Walk Angular mean ±angular variance	Walk Rayleigh P-value	Watson–Williams F-value (d.f.)	Watson–Williams P-value	Benjamini–Hochberg P-value
t min. horizontal fin angle (deg)		7	87.73±78.95	0.0056	90.32±85.26	0.0345	148.39 (1,101)	<0.0001*	<0.0001*
t max. horizontal fin angle (deg)		7	213.33±81.12	0.0022	209.97±82.65	0.0346	116.52 (1,111)	<0.0001*	<0.0001*
t burst 1 onset (deg)	Adductor	3	61.45±98.51	0.6663	321.41±80.62	0.6657	n/a	n/a	n/a
	Abductor	3	45.51±102.47	0.8125	48.84±11.45	0.0273	n/a	n/a	n/a
t burst 1 offset (deg)	Adductor	3	175.61±105.46	0.8833	47.40±95.15	0.8767	n/a	n/a	n/a
	Abductor	3	103.05±101.80	0.7934	165.04±42.68	0.2165	n/a	n/a	n/a
t burst 2 onset (deg)	Adductor	3	10.15±76.30	0.1686	97.12±67.59	0.2677	n/a	n/a	n/a
	Abductor	3	111.98±97.75	0.7139	236.30±62.55	0.7106	n/a	n/a	n/a
t burst 2 offset (deg)	Adductor	3	89.65±79.58	0.2066	137.81±84.40	0.6769	n/a	n/a	n/a
	Abductor	3	152.39±97.89	0.7182	31.82±0.14	0.1362	n/a	n/a	n/a
t max. burst 1 amplitude (deg)	Adductor	3	124.27±97.77	0.6552	281.46±79.23	0.6430	n/a	n/a	n/a
	Abductor	3	85.42±88.76	0.4061	87.32±27.62	0.0480	n/a	n/a	n/a
t max. burst 2 amplitude (deg)	Adductor	3	58.75±70.02	0.0747	160.39±74.78	0.3928	n/a	n/a	n/a
	Abductor	3	152.48±102.78	0.8477	348.35±8.92	0.1970	n/a	n/a	n/a

Numerator and denominator d.f. are given in parentheses after F-values. Significant differences are indicated with an asterisk. When Rayleigh's test did not indicate significant directionality for both swimming and walking conditions, Watson–Williams tests were not performed.

Here, we have demonstrated short-term changes in neuromuscular function in the form of modulation of magnitude and timing of muscle activity in *P. senegalus* raised in an aquatic environment. Given the alterations of skeletal morphology and muscle fibre type observed in *P. senegalus* raised on land (Standen et al., 2014; Du and Standen, 2017), it remains to be seen whether terrestrialized individuals would modulate motor unit recruitment in the same way. The altered fibre type ratios in terrestrialized individuals may result in alterations to the shapes of muscle bursts or in shifts in the preferential use of one fibre type over another. Furthermore, whether other physiological aspects of the muscles, such as force–length properties, also demonstrate plasticity in response to terrestrialization remains to be explored. Applying the techniques used in this study, in addition to techniques like wavelet analysis and *in vitro* studies of muscle contractile properties, will greatly improve our understanding of the challenges of the locomotor transition between water and land and muscle plasticity in general.

Conclusions

The data presented here demonstrate significant functional modulation of fin and body muscle in *P. senegalus* moving in water and on land. In most positions along the body, *P. senegalus* appears to modulate locomotor behaviour primarily through changes in absolute duration and timing of activity relative to kinematic movements. However, in the secondary bursts of the fin muscles and in the primary burst of the muscle in the middle of the body, the magnitude of motor unit recruitment is also modulated. In these locations, muscle activation changes from a more constant, moderate level of motor unit recruitment when swimming, to more intermittent, high-intensity recruitment when walking. These changes in activity pattern suggest that the greater locomotor demands of walking may be met predominantly through forces generated by body musculature located half-way down the length of the fish, with the fin functioning primarily to support the body through antagonistic muscle activity. The physiological consequences of these shifts in muscle activation profile and how these may change in terrestrialized *P. senegalus* are certain to be highly fruitful areas of future investigation.

References

Alexander, R. M. N. (1977). Allometry of the limbs of antelopes (Bovidae). *J. Zool.* **183**, 125-146.

Azizi, E. (2014). Locomotor function shapes the passive mechanical properties and operating lengths of muscle. *Proc. Biol. Sci.* **281**, 20132914.

Benjamini, Y. and Hochberg, Y. (1995). Controlling the false discovery rate: a practical and powerful approach to multiple testing. *J. R. Statist. Soc. B* **57**, 289-300.

Biewener, A. A. and Gillis, G. B. (1999). Dynamics of muscle function during locomotion: accommodating variable conditions. *J. Exp. Biol.* **202**, 3387-3396.

Bravata, D. M. and Olkin, I. (2001). Simple pooling versus combining in meta-analysis. *Eval. Health Prof.* **24**, 218-230.

Carlson-Kuhta, P., Trank, T. V. and Smith, J. L. (1998). Forms of forward quadrupedal locomotion. II. A comparison of posture, hindlimb kinematics, and motor patterns for upslope and level walking. *J. Neurophysiol.* **79**, 1687-1701.

Cartmill, M. (1985). Climbing. In *Functional Vertebrate Morphology* (ed. M. Hildebrand, D. M. Bramble, K. F. Liem and D. B. Wake), pp. 73-88. Cambridge, MA: Harvard University Press.

Daley, M. A. and Biewener, A. A. (2003). Muscle force–length dynamics during level versus incline locomotion: a comparison of *in vivo* performance of two guinea fowl ankle extensors. *J. Exp. Biol.* **206**, 2941-2958.

Du, T. Y. and Standen, E. M. (2017). Phenotypic plasticity of muscle fiber type in the pectoral fins of *Polypterus senegalus* reared in a terrestrial environment. *J. Exp. Biol.* **220**, 3406-3410.

Field, A. (2009). *Discovering Statistics Using SPSS*. London: Sage Publications Ltd.

Foster, K. L. and Higham, T. E. (2014). Context-dependent changes in motor control and kinematics during locomotion: modulation and decoupling. *Proc. Biol. Sci.* **281**, 20133331.

Foster, K. L. and Higham, T. E. (2017). Integrating gastrocnemius force–length properties, *in vivo* activation and operating lengths reveals how *Anolis* deal with ecological challenges. *J. Exp. Biol.* **220**, 796-806.

Gabaldón, A. M., Nelson, F. E. and Roberts, T. J. (2001). Gastrocnemius muscle mechanics in turkeys during uphill and downhill running. *Amer. Zool.* **41**, 1448.

Gans, C. and de Vree, F. (1987). Functional bases of fiber length and angulation in muscle. *J. Morphol.* **192**, 63-85.

Gatesy, S. M. (1997). An electromyographic analysis of hindlimb function in *Alligator* during terrestrial locomotion. *J. Morphol.* **234**, 197-212.

Ghasemi, A. and Zahediasl, S. (2012). Normality tests for statistical analysis: a guide for non-statisticians. *Int. J. Endocrinol. Metab.* **10**, 486-489.

Gillis, G. B. (2000). Patterns of white muscle activity during terrestrial locomotion in the American eel (*Anguilla rostrata*). *J. Exp. Biol.* **203**, 471-480.

Gillis, G. B. and Biewener, A. A. (2000). Hindlimb extensor muscle function during jumping and swimming in the toad (*Bufo marinus*). *J. Exp. Biol.* **203**, 3547-3563.

Gillis, G. B. and Biewener, A. A. (2002). Effects of surface grade on proximal hindlimb muscle strain and activation during rat locomotion. *J. Appl. Physiol.* **93**, 1731-1743.

Gillis, G. B. and Blob, R. W. (2001). How muscles accommodate movement in different physical environments: aquatic vs. terrestrial locomotion in vertebrates. *Comp. Biochem. Physiol. A Molec. Integr. Physiol.* **131**, 61-75.

Hedrick, T. L. (2008). Software techniques for two- and three-dimensional kinematic measurements of biological and biomimetic systems. *Bioinspir. Biomim.* **3**, 034001.

Higham, T. E. and Jayne, B. C. (2004). *In vivo* muscle activity in the hindlimb of the arboreal lizard, *Chamaeleo calyptratus*: general patterns and the effects of incline. *J. Exp. Biol.* **207**, 249-261.

Hodson-Tole, E. and Wakeling, J. M. (2009). Motor unit recruitment for dynamic tasks: current understanding and future directions. *J. Comp. Physiol. B* **179**, 57-66.

Holt, N. C. and Azizi, E. (2016). The effect of activation level on muscle function during locomotion: are optimal lengths and velocities always used? *Proc. Biol. Sci.* **283**, 20152832.

Koh, T. J. (1997). Regulation of sarcomere number in the growing rabbit tibialis anterior. PhD dissertation, University of Calgary, Calgary, AB, Canada.

Koh, T. J. and Herzog, W. (1998). Excursion is important in regulating sarcomere number in the growing rabbit tibialis anterior. *J. Physiol.* **508**, 267-280.

Lieber, R. L. and Ward, S. R. (2011). Skeletal muscle design to meet functional demands. *Philos. Trans. R. Soc. Lond. B. Biol. Sci.* **366**, 1466-1476.

Loeb, G. E. and Gans, C. (1986). The organization of muscle. In *Electromyography for Experimentalists*, pp. 25-43. London: University of Chicago Press.

Lynn, R. and Morgan, D. L. (1994). Decline running produces more sarcomeres in rat vastus intermedius muscle fibers than does incline running. *J. Appl. Physiol.* **77**, 1439-1444.

McDonald, J. H. (2014). Multiple comparisons. In *Handbook of Biological Statistics*, pp. 257-263. Baltimore, MD: Sparky House Publishing.

Payne, R. C., Crompton, R. H., Isler, K., Savage, R., Vereecke, E. E., Günther, M. M., Thorpe, S. K. S. and D'Août, K. (2006). Morphological analysis of the hindlimb in apes and humans. II. Moment arms. *J. Anat.* **208**, 725-742.

Pette, D. and Staron, R. S. (2000). Myosin isoforms, muscle fiber types, and transitions. *Microsc. Res. Tech.* **50**, 500-509.

Preuschoft, H. (2002). What does 'arboreal locomotion'mean exactly and what are the relationships between 'climbing', environment and morphology? *Z. Morphol. Anthropol.* **83**, 171-188.

Rassier, D. E., MacIntosh, B. R. and Herzog, W. (1999). Length dependence of active force production in skeletal muscle. *J. Appl. Physiol.* **86**, 1445-1457.

Reilly, S. M. (1995). Quantitative electromyography and muscle function of the hind limb during quadrupedal running in the lizard *Sceloporus clarkii*. *Zool. Anal. Comp. Syst.* **98**, 263-277.

Roberts, T. J. and Gabaldón, A. M. (2008). Interpreting muscle function from EMG: lessons learned from direct measurements of muscle force. *Integr. Comp. Biol.* **48**, 312-320.

Roberts, T. J., Higginson, B. K., Nelson, F. E. and Gabaldón, A. M. (2007). Muscle strain is modulated more with running slope than speed in wild turkey knee and hip extensors. *J. Exp. Biol.* **210**, 2510-2517.

Roberts, T. J., Marsh, R. L., Weyand, P. G. and Taylor, C. R. (1997). Muscular force in running turkeys: the economy of minimizing work. *Science* **275**, 1113-1115.

Sacks, R. D. and Roy, R. R. (1982). Architecture of the hind limb muscles of cats: functional significance. *J. Morphol.* **173**, 185-195.

Schiaffino, S. and Reggiani, C. (2011). Fiber types in mammalian skeletal muscles. *Physiol. Rev.* **91**, 1447-1531.

Standen, E. M., Du, T. Y. and Larsson, H. C. E. (2014). Developmental plasticity and the origin of tetrapods. *Nature* **513**, 54-58.

Standen, E. M., Du, T. Y., Laroche, P. and Larsson, H. C. E. (2016). Locomotor flexibility of *Polypterus senegalus* across various aquatic and terrestrial substrates. *Zoology* **119**, 447-454.

Thompson, J. T., Shelton, R. M. and Kier, W. M. (2014). The length–force behavior and operating length range of squid muscle vary as a function of position in the mantle wall. *J. Exp. Biol.* **217**, 2181-2192.

Wakeling, J. M. (2004). Motor units are recruited in a task-dependent fashion during locomotion. *J. Exp. Biol.* **207**, 3883-3890.

Wakeling, J. M., Kaya, M., Temple, G. K., Johnston, I. A. and Herzog, W. (2002). Determining patterns of motor recruitment during locomotion. *J. Exp. Biol.* **205**, 359-369.

Wilson, A. and Lichtwark, G. (2011). The anatomical arrangement of muscle and tendon enhances limb versatility and locomotor performance. *Philos. Trans. R. Soc. Lond. B. Biol. Sci.* **366**, 1540-1553.

Zar, J. H. (1999). *Biostatistical Analysis*. Upper Saddle River, NJ: Prentice Hall.

Zierath, J. R. and Hawley, J. A. (2004). Skeletal muscle fiber type: influence on contractile and metabolic properties. *PLoS Biol.* **2**, e348.

Table S1. Electrode implantation locations and number of swimming and walking strokes with both kinematic and muscle activity data for each individual. Numbers corresponding to electrode location along the body correspond with locations in Figure 1. R, right; L, left.

Fish ID	# strokes		Electrode Locations	
	Swimming	Walking	Fin	Body
3	6	0		1R,3R,5R,1L,3L,5L
4	5	12		1R,3R,5R,1L,3L,5L
5	5	6		1L,2L,3L,4L,5L
6	7	0	adductor/abductor	1R,3R,5R,1L,3L,5L
9	7	4	adductor	1R,2R,3R,4R,5R
10	5	4	abductor	1L,2L,3L,4L,5L
11	7	6	adductor	1L,2L,3L,4L,5L
12	15	17		3L,1R,3R,5R
13	8	4	abductor	1R,2R,3R,4R,5R

Dataset 1

Click here to Download Dataset 1